JAAS

Accepted Manuscript

This is an *Accepted Manuscript*, which has been through the Royal Society of Chemistry peer review process and has been accepted for publication.

Accepted Manuscripts are published online shortly after acceptance, before technical editing, formatting and proof reading. Using this free service, authors can make their results available to the community, in citable form, before we publish the edited article. We will replace this *Accepted Manuscript* with the edited and formatted *Advance Article* as soon as it is available.

You can find more information about *Accepted Manuscripts* in the Information for Authors.

Please note that technical editing may introduce minor changes to the text and/or graphics, which may alter content. The journal's standard Terms & Conditions and the Ethical guidelines still apply. In no event shall the Royal Society of Chemistry be held responsible for any errors or omissions in this *Accepted Manuscript* or any consequences arising from the use of any information it contains.

ROYAL SOCIETY OF CHEMISTRY

www.rsc.org/jaas

Journal Name

ARTICLE

Analyses of ions doping profiles in Yb-doped fiber preforms using laser-induced breakdown spectroscopy

Received 00th January 20xx,
Accepted 00th January 20xx

DOI: 10.1039/x0xx00000x

www.rsc.org/

Jiaming Li, Lianbo Guo, Nan Zhao, Qimeng Chen, Baoye Wu, Yibo Wang, Xiangyou Li*, Jinyan Li, Xiaoyan Zeng, Yongfeng Lu

Abstract Ions doping profiles are one of the most important characteristics in Yb-doped fibers but it is hard to realize rapid, in-situ, and online analyses. A laser-induced breakdown spectroscopy (LIBS) system was set up to analyze ions doping profiles in Yb-doped fiber preforms. However, the laser-induced irregular cracking occurred on the preform surfaces and generated outliers in the Yb maps affected the analytical effects. An algorithm of a self-adaptive median filter (SAMF) was introduced to modify the maps. The results of LIBS mapping assisted by SAMF clearly described the doping profiles of step-wise and central dip. The energy dispersive X-ray spectroscopy (EDS) and the X-ray fluorescence (XRF) techniques were used to validate the analytical results. This study provides a rapid, in-situ, and online approach for ions doping profiles analyses in Yb-doped fibers.

1. Introduction

Since being invented in the 1980s,[1] Yb-doped fiber has become a research hotspot in fiber laser,[2] optical amplifier,[3] and fiber sensor[4] investigations. In the Yb-doped fiber, Ytterbium is the key ion that provides light amplification. Other co-doped ions participate in optimizing the fiber performance.[5] For example, Aluminium ion decreases the Yb ions agglomeration and improves the efficiency.[6] As one of its most important characteristics, ions doping profiles of these ions have been proved to greatly affect, even determine the fiber mode area, slope efficiency, environmental response, and output beam quality.[7-9] Therefore, it is of great importance to analyze the ions doping profiles in fiber preforms to assess the quality of fiber preforms and predict the fiber performance before fiber drawing. Conventionally, ions doping profiles are estimated indirectly by measuring the refractive index profiles one dimensionally, which can only obtain the amount of all the ions, instead of the doping profiles of each element. Other analytical methods, such as energy dispersive X-ray spectroscopy (EDS), electron probe microanalysis (EPMA), and X-ray fluorescence, could also be used to analyze the ytterbium of fiber preforms. However, due to their complex sample preparation, long consuming time, vacuum, and liquid-nitrogen cooling, most of them are only applied in laboratories, but not in the industries. To overcome these drawbacks, much effort has been expended to search for new techniques for achieving rapid and convenient analyses in fiber preforms to satisfy analytical requirements in industry.

Wuhan National Laboratory for Optoelectronics (WNLO), Huazhong University of Science and Technology, Wuhan, Hubei 430074, P. R. China.
E-mail: xyli@mail.hust.edu.cn; Fax: +86-27-87541423; Tel: +86-27-87541423

Laser-induced breakdown spectroscopy (LIBS) is a laser-ablation-based method of spectrochemistry. It can realize rapid, in-situ, and online analyses in open air,[10-12] without complex equipment maintenance and sample preparation. By scanning the area and analyzing the spectra of each point, elemental distribution maps can be acquired.[13, 14] As a versatile technique in the field of elemental analysis, LIBS mapping has attracted more and more attention since H.J. Häkkänen *et al.*[15] discovered its great potential in 1995. J. Kaiser *et al.*[16, 17] verified the high reliability of LIBS mapping by comparing it with laser ablation inductively coupled plasma mass spectrometry (LA-ICP-MS). I. Lopez-Quintas *et al.*[18] demonstrated its capability for 3D characterization by scanning complex steel in surface and in depth. G. Nicolas *et al.*[19] realized 3D mapping on a nonflat sample, which enhanced LIBS mapping adaptability of complex surfaces. Due to its capability, reliability, and adaptability, LIBS mapping has been widely applied in different fields. For example, F. Boué-Bigne[20, 21] introduced LIBS mapping for rapid segregation detection in the steel industry. X. Wang *et al.*[22] utilized LIBS mapping to analyze multielemental distribution in different phases of nuclear waste in glass–ceramics. V. Motto-Ros *et al.*[23] determined the cause of heavy metal Gd deposition in urinary systems by LIBS mapping on a murine kidney.

The works mentioned above have proved that LIBS mapping is a suitable technique for elemental distribution analyses. Hence, it is feasible to analyze ions distribution in fiber preforms, namely ions doping profiles. However, because the preform surface is ablated by the laser pulse, irregular laser-induced cracking occurs and generates outliers on the chemical maps, results in the difficulty of analysing and few studies have focused on LIBS mapping on fiber preforms at present.

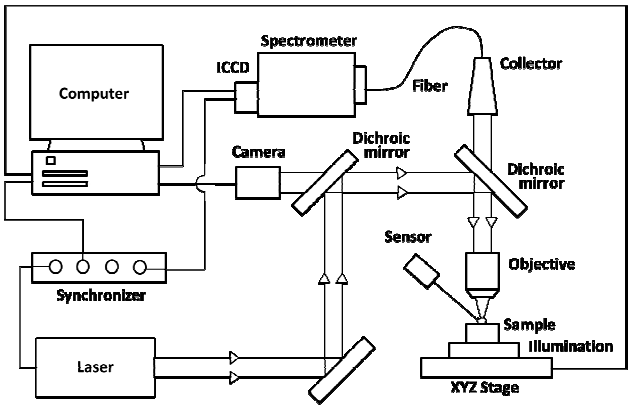

Fig. 1. Schematic diagram of the experimental setup.

In this work, a self-adaptive median filter (SAMF) is introduced to improve the analytical effects of Yb and Al doping profiles in fiber preforms due to its simplicity and capability for impulse noise elimination.[24, 25] Furthermore, the analytical results were validated by the EDS and XRF techniques.

2. Experimental methods

2.1 Experimental setup

The schematic diagram of the LIBS setup is shown in Figure 1. A Q-switched Nd:YAG laser (Beamtech, Nimma 400, pulse duration of 8 ns) operating at 532 nm, 3 Hz, and 300 μJ was used as the ablation source. The laser beam was reflected by a reflect mirror and two dichroic mirrors and then focused onto the sample surface by a 5× objective to generate plasmas. The light emission from the plasmas was collected by a light collector (Ocean Optics, 84-UV-25, wavelength range of 200-2000 nm) and coupled with a Czerny-Turner spectrometer (Princeton Instruments, SCT320, grating of 1200 lines per mm) through a multicore fiber (Avantes). An intensified charge-coupled device (ICCD) (Princeton Instruments, Max3) was installed on the spectrometer to record the spectra. The sample was illuminated by a plane light under the sample. A motorized XYZ stage was used to move the sample and was monitored by a CCD camera. The laser and the ICCD were synchronized by a digital synchronizer (Stanford Instruments, DG535).

An environmental scanning electron microscope (FEI, ESEM Quanta 200) equipped with an energy dispersive spectrometer was used to validate the LIBS analyses. The fiber preform samples were preprocessed with a carbon coating to improve the conductivity before the EDS detection.

An X-ray fluorescence probe (EDAX, EAGLE III) was also used as reference. The X-ray spot on the fiber preform samples was 100 μm.

2.2 Fiber preform samples

As shown in Figure 2, two Yb-doped fiber preforms with aluminum (Al) co-doped were used in this work. They were fabricated by the modified chemical-vapor deposition (MCVD) and the solution doping technique. The matrices of the fiber

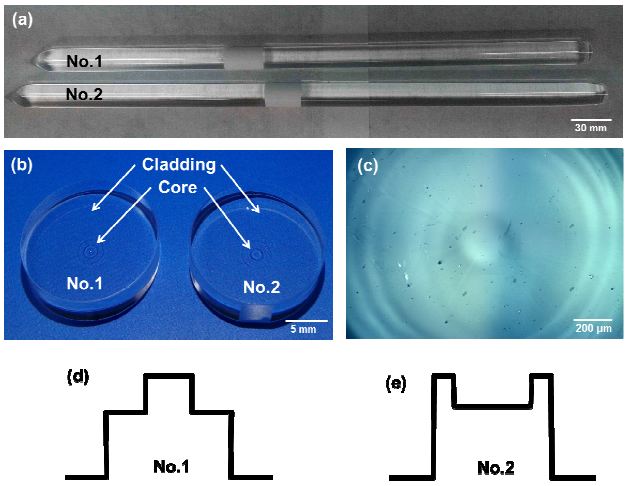

Fig. 2. The images of the fiber preforms. (a) Full view of the fiber preforms; (b) the fiber preform samples after being cut; (c) the microscope image of fiber preform core; (d) general doping profile sketch of sample No. 1; (e) general doping profile sketch of sample No. 2.

samples were silica. The Yb^{3+} concentration of the two samples were about 0.5 and 0.4 wt%, respectively. The Al^{3+} concentration of the two samples were about 2 and 1 wt%, respectively.

The two fiber preform samples were about 400 mm in length and 16 mm in diameter, as shown in Figure 2(a). A small piece was cut off from each sample and polished in Fig. 2(b). The core shown in Fig. 2(c) was the area analyzed. The doping profiles of the two samples were generally designed to be step-wise (sample No. 1) and central dip (sample No. 2). The ideal profiles of these fiber preforms are shown in Fig. 2(d) and 2(e).

2.3 SAMF algorithm

The median filter is a nonlinear filter based on the taxis statistical theory, proposed by J.W. Tukey.[26] It was convinced to be one of the most capable tools to eliminate impulse noise with preserving image edges.[27] SAMF is a modified median filter, which is added with an impulse noise detection into a conventional median filter. It can both modify bad points corrupted by impulse noise and reserve good points.[28] The SAMF algorithm can be described by

$$M(m,n)=\text{Median}[X(m-k:m+k,n-k:n+k)], \quad (1)$$

$$\text{and} \quad Y(m,n)=\begin{cases} M(m,n), & X(m,n)=X_{\max} \text{ or } X_{\min} \\ X(m,n), & \text{others} \end{cases}. \quad (2)$$

In Equation 1, X represents the original $M\times N$ matrix; M is the matrix modified by the conventional median filter. In Equation 2, X_{max} and X_{min} are the maximum and minimum values of the window $X(m\text{-}k : m\text{+}k , n\text{-}k : n\text{+}k)$ centered on the corresponding point $X(m,n)$; Y represents the data matrix output from SAMF. In the impulse noise detection, if the point value in X is the extremum value of the window, the point is regarded as a bad point corrupted by impulse noise; otherwise, the point is a good point. The bad points are replaced by the M, while the good points are reserved the original values in the X.

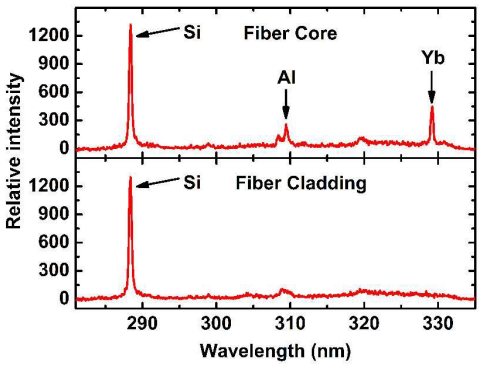

Fig. 3. The spectra of the fiber preform. (a) Spectrum of the core; (b) spectrum of the cladding.

3. Results and discussion

3.1 The LIBS spectra of fiber preforms

As shown in Figure 3, LIBS spectra of Yb II 328.9 nm, Al I 309.3 nm, and Si I 288.1 nm from the core and the cladding of the fiber preform were acquired at a gate delay of 100 ns and a gate width of 1 μs. Obviously, the core was doped with Yb^{3+} and Al^{3+}, while the cladding was pure silica.

3.2 Ions doping profiles before SAMF processing

The normalized ratios of Yb II 328.9 nm/Si I 288.1 nm and Al I 309.3 nm/Si I 288.1 nm maps are shown in Figure 4. The spatial resolution was 30 μm and the consuming time was about 15 minutes for each sample. The cores and the claddings are distinguished clearly from the Yb maps in Fig. 4(a) and 4(b). However, the doping profile details of the step-wise and the central dip are hard to be described because several harmful outliers seriously corrupted the maps. This is a serious problem in LIBS mapping on fiber preforms.

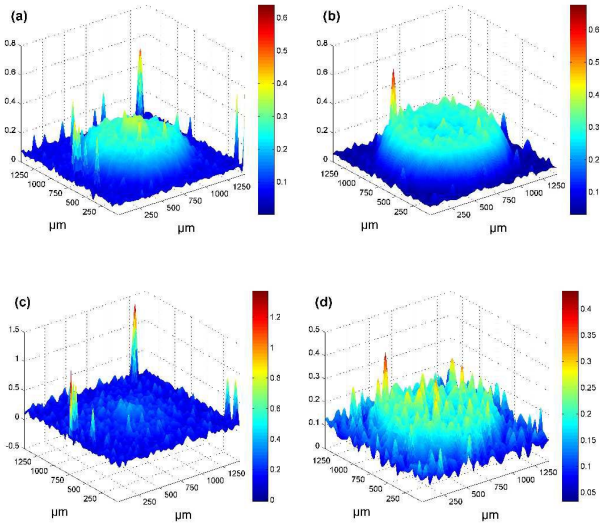

Fig. 4. The normalized ratios maps of Yb II 328.9 nm/Si I 288.1 nm of sample No.1 (a) and sample No.2 (b) before SAMF processing; the normalized ratios maps of Al I 309.3 nm/Si I 288.1 nm of sample No.1 (c) and sample No.2 (d) before SAMF processing.

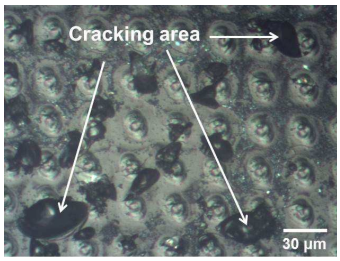

Fig.5. The surface images of the cracks on the fiber preform by a microscope.

To further investigate the reason for the outlier formation on the maps, the scanned areas were observed by a microscope. Figure 5 shows the surface images of the scanned area. From Fig. 5, the laser-induced irregular cracking was clearly found on the surface, and these cracks influenced the spectral intensity of the analyzed areas, which resulted in the formation of the outliers on the maps.

3.3 Testing SAMF by simulated maps

In this work, SAMF was used to overcome the problem of impulse noise in the Yb and Al maps. Before the four maps in Fig. 4 were input into SAMF, the capability of SAMF in eliminating impulse noise in the images of doping profiles was evaluated. Four typical maps of doping profiles in Figure 6 were simulated to participate in the evaluation. Firstly, the original maps were corrupted by impulse noise of different degrees (1-50%); secondly, the corrupted maps were input SAMF and the denoised maps were output; finally, the original maps and the denoised maps were compared. Such objective criteria as the mean square error (MSE) and the mean absolute error (MAE) were calculated to evaluate the achieved results of noise elimination and signal preservation[29, 30], respectively. The MSE and MAE are mathematically given by[24]

$$\mathrm{MSE} = \frac{\sum_{m=1}^{M}\sum_{n=1}^{N}\left[P(m,n)-Q(m,n)\right]^2}{M\times N}, \quad (3)$$

$$\mathrm{MAE} = \frac{\sum_{m=1}^{M}\sum_{n=1}^{N}\left|P(m,n)-Q(m,n)\right|}{M\times N}. \quad (4)$$

P and *Q* represent the original map and the denoised map, respectively. The MSE and the MAE in the four maps were calculated in Figure 7. The low MSE and MAE demonstrated good noise elimination in Fig. 7(a) and signal preservation in Fig.7 (b).

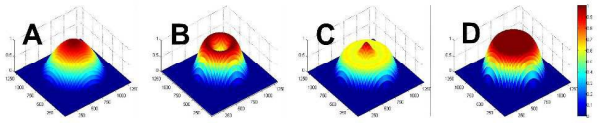

Fig.6. Four simulated doping profiles: quadratic function (A), central dip (B), central peak (C), and flattened gaussian (D).

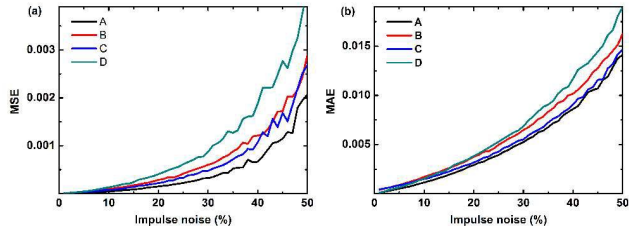

Fig.7. The MSE (a) and MAE (b) of SAMF denoising operation in the four simulated doping profiles.

3.4 Ions doping profiles after SAMF processing

The Yb and Al maps of the fiber preform samples were modified by the SAMF. The modified maps were obviously improved, as shown in Figure 8. The doping profiles of the step-wise can be clearly recognized in Fig. 8(a) and 8(c). The first step lowly doped in the outer core was about 1000 μm in diameter, and the second step highly doped in the inner core was about 300 μm in diameter. The ratios of doping content between the two steps were about 0.75 in Yb and 0.45 in Al. The doping profile of the central dip can also be clearly recognized in Fig. 8(b) and 8(d). The core was about 1200 μm in diameter. Compared with the edge area of the core, the interior area was less doped. At 100 μm in the center of Fig. 8 (b), a peak exists in Yb maps, which was harmful to expanding the mode area in the large-mode fiber.

3.5 Validation with EDS and XRF

To validate the results, the fiber preform samples were line-scanned across the middle of the cores using the EDS and

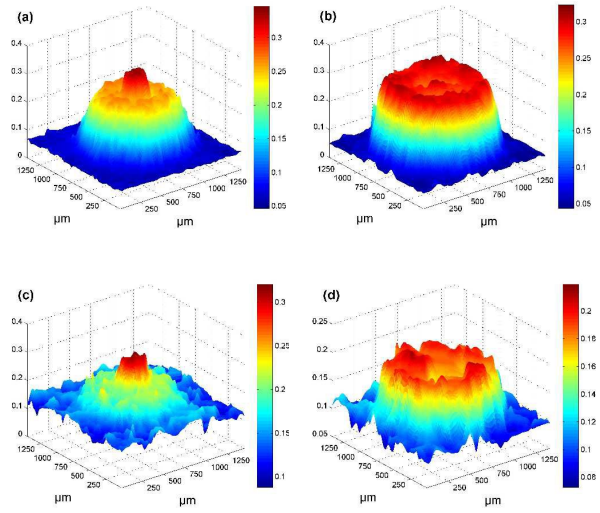

Fig. 8. The maps of Yb II 328.9 nm/Si I 288.1 nm of sample No.1 (a) and sample No. 2 (b) after SAMF processing; the maps of Al I 309.3 nm/Si I 288.1 nm of sample No.1 (c) and sample No. 2 (d) after SAMF processing.

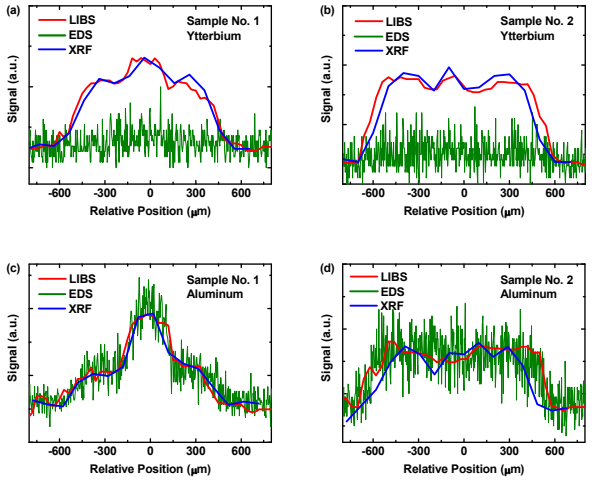

Fig. 9. Comparison of LIBS (red lines), EDS (green lines), and XRF (blue lines). (a) Yb in sample No. 1; (b) Yb in sample No. 2; (c) Al in sample No. 1 (d) Al in sample No. 2.

XRF technique. EDS has a high space-resolution but low sensitivity; XRF has a low space-resolution but high sensitivity. Compared with them, LIBS has a median space-resolution and high sensitivity. LIBS line-scanning datas were obtained by extracting datas from Fig. 8. As shown in Fig. 9, the results of Yb and Al in these three techniques agreed well, except the Yb in EDS. The reason for the exception of the Yb in EDS is that the EDS couldn't get Yb signal due to its low sensitivity for low concentration elements. This result proved that the doping profiles analyzed by LIBS were reliable. Furthermore, the analytical time of LIBS was 1/40 of EDS and 1/80 of XRF, which didn't include the vacuum time before analyses in EDS and XRF. LIBS assisted with SAMF provides a rapid tool for doping structure profiling in the fiber preforms.

4. Conclusions

In this work, the Yb and Al doping profiles of fiber preforms were analyzed by the LIBS mapping technique. To overcome the problems of irregular cracking and outliers in the maps, the SAMF was introduced to modified analyses of the doping profiles. The spatial resolution and analytical time were 30 μm and 15 minutes, respectively. The results of the methods were validated by EDS and XRF techniques. Through LIBS assisted by SAMF, the quality of the fiber preforms was assessed, and the performance of the fiber was predicted before fiber drawing. The results of this study provide a rapid and capable approach for analysing ions doping profiles in fiber preforms. A further study could improve spatial resolution by using UV laser ablation and shorten the consuming time by increasing the repetition rate of the laser device.

Acknowledgements

This research was financially supported by the National Special Fund for the Development of Major Research Equipment and Instruments (No. 2011YQ160017), the National Natural Science Foundation of China (No. 61575073, 51429501, and 61378031) , and the Fundamental Research Funds for the Central Universities (HUST: 2015TS075).

The authors would like to thank Prof. Nengli Dai and Dr. Yingbo Chu of Fiber Laser Technology Group (FLTG) in Wuhan National Laboratory for Optoelectronics (WNLO), and Analytical and Testing Center in Huazhong University of Science and Technology (HUST).

Notes and references

1. S. Poole, D. N. Payne and M. E. Fermann, *Electron. Lett*, 1985, 21, 737-738.
2. Y. e. Jeong, J. Sahu, D. Payne and J. Nilsson, *Opt. Express*, 2004, 12, 6088-6092.
3. R. Paschotta, J. Nilsson, A. C. Tropper and D. C. Hanna, *IEEE Journal of quantum electronics*, 1997, 33, 1049-1056.
4. E. Maurice, S. A. Wade, S. F. Collins, G. Monnom and G. W. Baxter, *Appl. Opt.*, 1997, 36, 8264-8269.
5. M. J. Digonnet, *Rare-earth-doped fiber lasers and amplifiers, revised and expanded*, CRC press, 2001.
6. T. Kitabayashi, M. Ikeda, M. Nakai, T. Sakai, K. Himeno and K. Ohashi, 2006.
7. W. Wen-Liang, H. Liang-Jin, L. Jin-Yong, G. Shao-Feng and J. Zong-Fu, *Chinese Physics B*, 2014, 23, 094207.
8. J. R. Marciante, R. G. Roides, V. V. Shkunov and D. A. Rockwell, *Opt. Lett.*, 2010, 35, 1828-1830.
9. M. Hotoleanu, M. Söderlund, D. Kliner, J. Koplow, S. Tammela and V. Philipov, 2006.
10. C. M. Li, Z. M. Zou, X. Y. Yang, Z. Q. Hao, L. B. Guo, X. Y. Li, Y. F. Lu and X. Y. Zeng, *J. Anal. At. Spectrom.*, 2014, 29, 1432-1437.
11. R. Noll, *Laser-induced breakdown spectroscopy*, Springer, 2012.
12. Z. Wang, T. B. Yuan, Z. Y. Hou, W. D. Zhou, J. D. Lu, H. B. Ding and X. Y. Zeng, *Frontiers of Physics*, 2014, 9, 419-438.
13. T. Kim, C. Lin and Y. Yoon, *J. Phys. Chem. B*, 1998, 102, 4284-4287.
14. V. Pinon, M. Mateo and G. Nicolas, *Appl. Spectrosc. Rev.*, 2013, 48, 357-383.
15. H. J. Häkkänen and J. E. I. Korppi-Tommola, *Appl. Spectrosc.*, 1995, 49, 1721-1728.
16. J. Kaiser, M. Galiová, K. Novotný, R. Červenka, L. Reale, J. Novotný, M. Liška, O. Samek, V. Kanický and A. Hrdlička, *Spectrochim. Acta, Part B*, 2009, 64, 67-73.
17. K. Novotný, J. Kaiser, M. Galiová, V. Konečná, J. Novotný, R. Malina, M. Liška, V. Kanický and V. Otruba, *Spectrochim. Acta, Part B*, 2008, 63, 1139-1144.
18. I. Lopez-Quintas, M. Mateo, V. Piñon, A. Yañez and G. Nicolas, *Spectrochim. Acta, Part B*, 2012, 74, 109-114.
19. G. Nicolas, M. Mateo and V. Pinon, *J. Anal. At. Spectrom.*, 2007, 22, 1244-1249.
20. F. Boué-Bigne, *Spectrochim. Acta, Part B*, 2008, 63, 1122-1129.
21. F. Boué-Bigne, *Spectrochim. Acta, Part B*, 2014, 96, 21-32.
22. X. Wang, V. Motto-Ros, G. Panczer, D. De Ligny, J. Yu, J. Benoit, J. Dussossoy and S. Peuget, *Spectrochim. Acta, Part B*, 2013, 87, 139-146.
23. V. Motto-Ros, L. Sancey, X. Wang, Q. Ma, F. Lux, X. Bai, G. Panczer, O. Tillement and J. Yu, *Spectrochim. Acta, Part B*, 2013, 87, 168-174.
24. A. K. Samantaray, 2014.
25. T. Chen, K. K. Ma and L. H. Chen, *Image Processing, IEEE Transactions on*, 1999, 8, 1834-1838.
26. J. W. Tukey, *Reading, Ma*, 1977, 231, 32.
27. T. Sun and Y. Neuvo, *Pattern Recog. Lett.*, 1994, 15, 341-347.
28. Z. Wang and D. Zhang, *IEEE Trans. Circuits-II*, 1999, 46, 78-80.
29. R. Lukac, *Pattern Recog. Lett.*, 2003, 24, 1889-1899.
30. C. S. Lee, Y. H. Kuo and P. T. Yu, *Fuzzy Sets and systems*, 1997, 89, 157-180.

This paper describes ion doping profiling in the Yb-doped fiber preforms using laser-induced breakdown spectroscopy assisted with self-adaptive median filter.